Liquid Crystals
Publication details, including instructions for authors and subscription information:
http://www.informaworld.com/smpp/title~content=t713926090

Correlated chain dynamics in the nematic phase of 4-cyano-4'-hexyloxybiphenyl

Ronald Y. Dong[ab]; G. Ravindranath[a]
[a] Department of Physics and Astronomy, Brandon University, Brandon, Canada [b] Physics Department, The University of Manitoba, Winnipeg, Canada

To cite this Article Dong, Ronald Y. and Ravindranath, G.(1994) 'Correlated chain dynamics in the nematic phase of 4-cyano-4'-hexyloxybiphenyl', Liquid Crystals, 17: 1, 47 — 63
To link to this Article: DOI: 10.1080/02678299408036549
URL: http://dx.doi.org/10.1080/02678299408036549

LIQUID CRYSTALS, 1994, VOL. 17, NO. 1, 47–63

Correlated chain dynamics in the nematic phase of 4-cyano-4′-hexyloxybiphenyl

by RONALD Y. DONG*†‡ and G. RAVINDRANATH†

† Department of Physics and Astronomy, Brandon University, Brandon, Manitoba, Canada R7A 6A9

‡ Physics Department, The University of Manitoba, Winnipeg, Manitoba R3T 2N2, Canada

(*Received 22 September 1993; accepted 12 October 1993*)

We report in this paper measurements of the Zeeman and Quadrupolar spin-lattice relaxation times at two different deuteron Larmor frequencies for the nematic phase of the perdeuteriated nematogen 6OCB. A model of correlated internal motion is used to account for both the quadrupolar splittings and the spectral densities of motion. The nematic mean field is constructed using the additive potential method, while the conformational transitions among the allowed configurations are described by a master equation. For modelling the quadrupolar splittings, we used 729 conformations, although this seemed impossible when the spectral densities were fitted by minimizing the sum of squares of per cent errors. The pentane effect has, therefore, been used to limit the size of the transition rate matrix in the master equation. We found that the dynamic model for liquid crystals proposed by one of us (1991, *Phys. Rev.* A, **43,** 4310) is essentially correct for 6OCB.

1. Introduction

Deuterium NMR spectroscopy is a powerful technique [1] for studying the orientational ordering and dynamics in liquid crystals. Normally a liquid crystalline molecule may be idealized by a rigid core with one or more flexible pendant hydrocarbon chains. Well-resolved quadrupolar doublets are commonly observed in deuterium NMR spectra of deuteriated liquid crystals [1]. Furthermore, partially relaxed deuterium spectra observed in multi-pulse experiments [2–4] also allow one to determine the Zeeman (T_{1Z}) and quadrupolar (T_{1Q}) spin-lattice relaxation times for various deuteriated atomic sites of a mesogen. Many workers [3–9] have recently employed this technique to extract spectral densities of motion $J_1(\omega_0)$ and $J_2(2\omega_0)$, where $\omega_0/2\pi$ is the Larmor frequency. The site, temperature and frequency dependences of $J_1^{(i)}(\omega)$ and $J_2^{(i)}(2\omega)$ can provide valuable information on dynamical processes in liquid crystals, which include molecular reorientation [10–12], internal rotations [13–15] and collective motions known as director fluctuations [16, 17].

Recently we have successfully modelled correlated internal motion in several nematogens such as *p*-methoxybenzylidene-*p*′-*n*-butylaniline (MBBA) [18] and 4-cyano-4′-*n*-pentylbiphenyl (5CB) [19, 20]. In an attempt to study internal motion in a liquid crystal of slightly longer chain length, we have chosen to study a perdeuteriated nematogen 4-cyano-4′-*n*-hexyloxy-d_{13}-biphenyl-d_8 (6OCB-d_{21}). Orientational order of

* Author for correspondence.

0267–8292/94 $10·00

6OCB has been examined by deuterium [21] and carbon-13 [22] NMR spectroscopy. Molecular rotation and ordering have also been studied [23] by measuring deuterium spectral densities and quadrupolar splittings for the deuterons on the two phenyl rings. There are two motional models that describe rotation of a symmetric top in a pseudo-potential of Maier–Saupe type. The small step rotational diffusion model [10] has been widely used in various investigations of liquid crystals. The rotational diffusion tensor of the molecule is diagonalized in a molecule-fixed frame when the rotational diffusion equation is solved. The choice of rotational diffusion tensor is, strictly speaking, appropriate for an isotropic liquid. Freed and co-workers [11] proposed an alternative model in which the rotational diffusion tensor is diagonalized in a laboratory frame defined by the director. The latter model has been extended [12] to give a 'third rate' model which takes into account fast rotation about the molecular long axis. Both Nordio's model and the third rate model were considered [23] by examining the relaxation data from the biphenyl core of 6OCB. It was concluded that data from the chain deuterons must first be collected, preferably at two different Larmor frequencies, before one can examine these motional models in detail. In this paper, we therefore report spectral density measurements at 15·3 and 46·05 MHz for all deuteriated sites of 6OCB-d_{21}, except for the deuterons on the cyano ring. There are 729 (3^6) conformations for the hexyloxy chain based on the rotational isomeric state (RIS) model for Flory [24]. We adopt an angle (θ) of 4° between the ring *para*-axis and the C_{ar}–O bond, and a realistic geometry [25] ($\angle CCH = 107{\cdot}5°$, $\angle HCH = 113{\cdot}6°$, $\angle CCC = 113{\cdot}5°$ and the dihedral angles $\phi = 0, \pm 112°$). We treat the O–C and C–O bonds, like a C–C bond, except the $\angle COC$ and their bond lengths are different; the bond lengths do not affect the calculations of quadrupolar splittings when the additive potential method is used [21, 26]. The biphenyl core that includes the C_{ar}–O bond (see figure 1 (*a*)) is assumed to be cylindrically symmetric. By modelling quadrupolar splittings, the interaction parameters in the potential of mean torque, X_a and X_{cc} for the core and a C–C bond segment, respectively, and the nematic order parameter $\langle P_2 \rangle$ for an 'average' conformer can be obtained. These parameters are needed to model reorientation and correlated internal motions.

In our study of 5CB [20], which has a similar molecular structure to 6OCB, we found that both Nordio's model and the third rate model could be successfully used to describe molecular reorientation in its nematic phase. For simplicity and time consideration in computation, the small step rotational diffusion model of Nordio is used in the present study. A decoupled model [14] is adopted to describe conformational transitions that are superimposed onto molecular rotations of an average conformer. Now the transition matrix that appears in the master rate equation has a relatively large dimension (729×729). The CPU time required to solve the master equation and to calculate internal correlation functions is about an hour on a Vax station. We found that the minimization routine [27] Amoeba employed in optimizing fits between experimental and theoretical spectral densities would take many days for each temperature. Thus the relaxation data may only be handled at present by limiting the number of allowed conformations in the hexyloxy chain. We chose to eliminate those conformations that contain the $g^{\pm}g^{\mp}$ linkages (those gave rise to the pentane effect), making a smaller transition matrix (297×297). This speeded up the computation time by a factor of seven, thus making optimizations feasible. In this paper, we report on such calculations, bearing in mind that the results must be preliminary in nature. The contribution from director fluctuations [17] to deuteron spin relaxation rates is assumed to be negligible in the MHz region used in the present study.

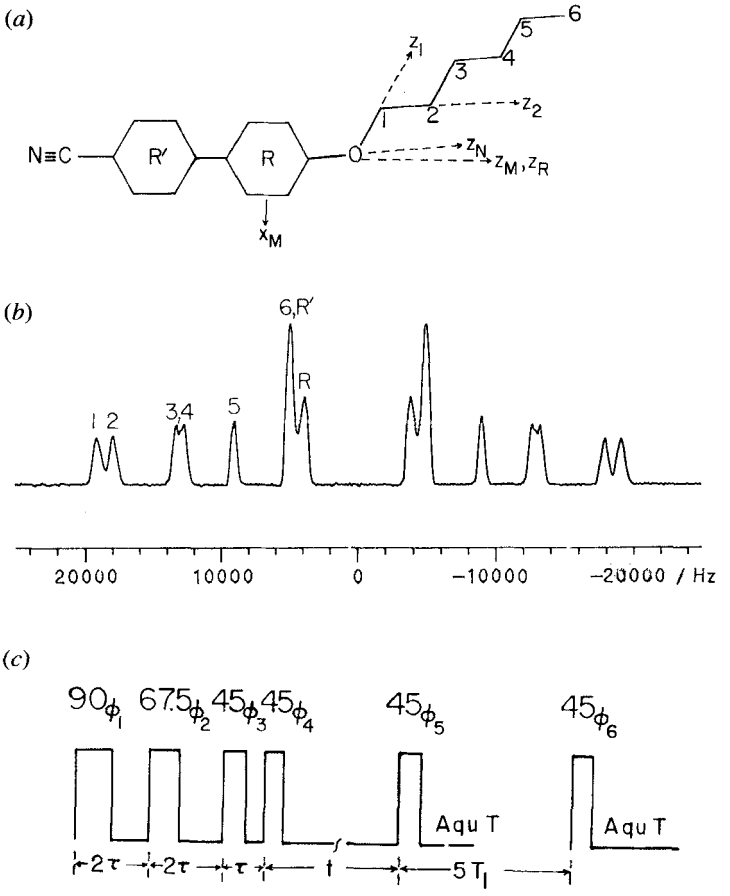

Figure 1. (*a*) Molecular structure of 6OCB, (*b*) a typical deuterium NMR spectrum with peak assignments and (*c*) modified broadband Jeener–Broekaert pulse sequence.

2. Theory

Since the T_{1Z} and T_{1Q} for spin $I = 1$ are given by the standard spin relaxation theory [28]

$$\left.\begin{aligned} T_{1Z}^{-1} &= J_1(\omega_0) + 4J_2(2\omega_0), \\ T_{1Q}^{-1} &= 3J_1(\omega_0), \end{aligned}\right\} \tag{1}$$

they can be used to separate the two spectral densities of motion $J_1(\omega_0)$ and $J_2(2\omega_0)$. The spectral density may be calculated by Fourier transforming the time autocorrelation function $G_{m_L}(t)$

$$J_{m_L}(m_L\omega) = \frac{3\pi^2}{2}(q_{CD})^2 \int_0^\infty G_{m_L}(t)\cos(m_L\omega t)\,dt, \tag{2}$$

where $q_{CD} = e^2qQ/h$, the quadrupolar coupling constant ($\eta = 0$ is assumed here).

In the docoupled model [14], the autocorrelation function for $m_L \neq 0$ can be written as

$$G_{m_L}(t) = \sum_{m_M} \sum_{m_\alpha} \sum_{m'_\alpha} D^2_{m_M m_\alpha}(\Omega_{MN}) D^{2*}_{m_M m'_\alpha}(\Omega_{MN}) \times g_{m_L m_M}(t) \langle D^2_{m_\alpha 0}(\Omega_{NQ}(0)) D^{2*}_{m'_\alpha 0}(\Omega_{NQ}(t)) \rangle, \quad (3)$$

where $g_{m_L m_M}(t)$, the correlation functions that describe the reorientation of an average conformer, are given by

$$g_{m_L m_M}(t) = \langle D^2_{m_L m_M}(\Omega_{LM}(0)) D^{2*}_{m_L m_M}(\Omega_{LM}(t)) \rangle - \langle D^2_{m_L m_M}(\Omega_{LM}) \rangle \times \langle D^{2*}_{m_L m_M}(\Omega_{LM}) \rangle, \quad (4)$$

while $\langle D^2_{m_\alpha 0}(\Omega_{NQ}(0)) D^{2*}_{m'_\alpha 0}(\Omega_{NQ}(t)) \rangle$ are internal correlation functions that describe the internal motion of the chain. $D^2_{m,m'}(\Omega)$ are the Wigner rotation matrix, the Euler angles Ω_{LM} transform between a molecular (M) frame on the average conformer and the laboratory (L) frame, the Ω_{NQ} give the orientation of a particular C–D bond in a molecular N frame in which the chain conformations are defined and Ω_{MN} define a time-independent transformation between the two molecular frames (see figure 1 (*a*) for various frames). The decoupled model of correlated internal motion has been described in detail [14].

In this section we outline the necessary formulae for discussion of the measured quadrupolar splittings and spectral densities of motion. The calculations of quadrupolar splittings [29] and spectral densities are merged into a single computer program (written in Pascal). This is achieved by modifying the previous spectral density program [19] based on a diamond lattice to include the procedures [29] for generating all conformations with a realistic geometry and for calculating orientations of a set of C–D bonds in the chain. For ease of computing, we use Amoeba to fit the quadrupolar splittings separately by minimizing the sum squared error f

$$f = \sum_i [S^{(i)}_{CD}(\text{expt}) - S^{(i)}_{CD}(\text{calc})]^2, \quad (5)$$

and the spectral density data by minimizing the sum squared per cent error F

$$F = \sum_{\omega_0} \sum_i \sum_{m_L} \left[\frac{J^{(i)}_{m_L}(\text{expt}) - J^{(i)}_{m_L}(\text{calc})}{J^{(i)}_{m_L}(\text{expt})} \times 100 \right]^2. \quad (6)$$

In modelling the quadrupolar splittings ($\Delta\nu_i$) of the C_i deuteron(s), we define the segmental order parameters $S^{(i)}_{CD}$ by

$$S^{(i)}_{CD} = 2\Delta\nu_i/(3q^{(i)}_{CD}), \quad (7)$$

where $q^{(i)}_{CD}$ is the quadrupolar coupling constant for the C_i deuteron and is taken as 168 and 185 kHz for the methylene and ring deuterons, respectively. Suppose that $S^{(n)}_{\alpha\beta}$ represents an order parameter tensor which describes the orientational order of the nth rigid conformer. Then in the principal axis (a, b, c) frame of the nuclear quadrupolar interaction, we have

$$S^{(i)}_{CD} = \sum_n p_{eq}(n) \left[S^{n,i}_{aa} + \frac{\eta^{(i)}}{3} (S^{n,i}_{bb} - S^{n,i}_{cc}) \right], \quad (8)$$

where the C–D bond is taken to be along the axis a (i.e. $q^{(i)}_{aa} \equiv q^{(i)}_{CD}$), $\eta^{(i)}$, the asymmetry parameter of the electric field gradient, is defined by

$$\eta^{(i)} = (q^{(i)}_{bb} - q^{(i)}_{cc})/q^{(i)}_{aa}, \quad (9)$$

and $p_{eq}(n)$ is the fraction of molecules in the nth conformation. The order parameter $S_{kk}^{n,i}(k = a, b \text{ or } c)$ can be evaluated in the principal (x, y, z) frame of the order parameter tensor for the nth conformer using

$$S_{kk}^{n,i} = \sum_{\alpha} S_{\alpha\alpha}^{n} \cos^2 \theta_{\alpha k}^{n,i}, \tag{10}$$

where $\theta_{\alpha k}^{n,i}$ denote angles between the principal k axis and the principal $\alpha\ (= x, y, z)$ axis. For the ring deuterons, η is taken as 0·064 [30], which is small but non-zero. For the methylene deuterons, $\eta = 0$ is a very good approximation and $S_{CD}^{(i)}$ is simply a weighted average of the segmental order parameters $S_{CD}^{n,i}$ for the C_i–D bond in the nth conformer

$$S_{CD}^{(i)} = \sum_{n} p_{eq}(n) S_{CD}^{n,i}. \tag{11}$$

Both $p_{eq}(n)$ and $S_{kk}^{n,i}$ can be calculated from the intramolecular energy $U_{int}(n)$ and the anisotropic part of the potential of mean torque $U_{ext}(n, \omega)$ for the nth conformer, where ω defines the orientation of the director in a molecule-fixed frame. The total energy $U(n, \omega)$ of a single molecule [24] in the nth conformer is the sum of $U_{int}(n)$ and $U_{ext}(n, \omega)$. The internal energy in an alkyl chain is assumed to depend on the number (N_g) of *gauche* linkages and the number $(N_{g^{\pm}g^{\mp}})$ of $g^{\pm}g^{\mp}$ linkages in the chain of the nth conformer

$$U_{int}(n) = N_g E_{tg} + N_{g^{\pm}g^{\mp}} E_{g^{\pm}g^{\mp}}, \tag{12}$$

where E_{tg} is the energy difference between a *gauche* $(g^{\pm})$ state and the *trans* (t) state in the three rotational isomeric states approximation. The $E_{g^{\pm}g^{\mp}}$ is the energy of forming a $g^{+}g^{-}$ or $g^{-}g^{+}$ linkage. The second term in equation (12) is normally less important and our splitting data for 6OCB appear to support this ($E_{g^{\pm}g^{\mp}}$ is set to zero as in [21]). We assume [21] that E_{tg}(OCCC) and E_{tg}(COCC) are identical to E_{tg}(CCCC). Now $p_{eq}(n)$ is simply given by integrating the single particle distribution function $f(n, \omega)$ over all orientations to give

$$p_{eq}(n) = \exp[-U_{int}^{(n)}/kT] Q_n / Z, \tag{13}$$

where Z is the conformational–orientational partition function

$$Z = \sum_{n} \exp[-U_{int}(n)/kT] Q_n, \tag{14}$$

and Q_n is the orientational partition function for the nth conformer

$$Q_n = \int \exp[-U_{ext}(n, \omega)/kT]\, d\omega. \tag{15}$$

In the additive potential method [21, 24], the total interaction tensor $\tilde{\varepsilon}^n$ of the nth conformer is constructed by adding, in a common molecular frame, the local interaction tensors $\varepsilon_{2,r}^{j}$ (j = aromatic core or C–C bond segment) which are assumed to be cylindrically symmetric ($\delta_{r,0}$). We use X_a and X_{cc} to denote the unique component of the core (which includes the C_{ar}–O bond) and of the C–C segmental interactions. In the principal frame of $\tilde{\varepsilon}^n$

$$U_{ext}(n, \omega) = -\varepsilon_{2,0}^{n} P_2(\cos\beta) - \varepsilon_{2,2}^{n} (3/2)^{1/2} \sin^2\beta \cos 2\gamma, \tag{16}$$

where the polar angles (β, γ) denote the direction of the director in this frame. The principal components of the order tensor for the nth rigid conformer $S_{\alpha\alpha}^{n}$ can now

be evaluated [31] in this principal axis system. We note that the total interaction tensor and the order tensor for a particular conformer share a common principal frame. To calculate $S_{CD}^{(i)}$ for the methylene deuterons, the orientation of the C_i–D bond ($\theta_{\alpha k}^{n,i}$) in the nth principal frame must first be obtained. This is achieved by transforming the C_i–D vector ($\mathbf{V}_{CD}$) through successive coordinates

$$\mathbf{V}_{CD}^{p} = R_{P,M}R_{M,N}R_{N,1}R_{1,2}\ldots R_{i-1,i}\mathbf{V}_{CD}, \tag{17}$$

where $R_{i-1,i}$ is a rotation matrix that transforms between the ith local frame and $(i-1)$th local frame, and $R_{P,M}$ is the rotation matrix that transforms between the molecular M frame (x_M, y_M, z_M) and the principal frame. For the ring deuterons, we may use the following to get $\theta_{\alpha k}^{n,i}$

$$\mathbf{V}_{k}^{p} = R_{P,M}\mathbf{V}_{k}, \tag{18}$$

where $\mathbf{V}_k$ represent the direction of the principal k ($= a, b, c$) axis in the (x_M, y_M, z_M) frame. For example,

$$\mathbf{V}_a = \begin{pmatrix} \cos 31° \\ \cos 90° \\ \cos 59° \end{pmatrix},$$

where the angle of 59° is assumed between the ring C–D bond and its *para*-axis in order to get better fits between the experimental and theoretical ring splittings, at least at low temperatures.

The transition matrix obeys the following master equation:

$$\frac{\partial p_{il_0}(t)}{\partial t} = \sum_{j=1}^{N} R_{ij}p_{jl_0}(t), \tag{19}$$

where $p_{jl_0}(t)$ is the conditional probability that the chain assumes conformation j at time t, when at $t=0$ the chain has the lth conformation, R_{ij} is the rate constant for the transition from conformation j to conformation i and $N=297$ is used here. R_{ij} is constructed based on transitions that take place through one-bond, two-bond or three-bond motion [32], with jump rate k_1, k_2 or k_3, respectively. Our two-bond motion is defined by [19]

$$\{ijklmno\} \rightarrow \{ijklmn'o'\}, \tag{20}$$

where { } denotes the orientations of the hexyloxy chain backbone. R_{ij} must satisfy the detailed-balance principle

$$R_{ij}p_{eq}(j) = R_{ji}p_{eq}(i), \tag{21}$$

and its diagonal elements are

$$R_{ii} = -\sum_{j\neq i} R_{ji}. \tag{22}$$

To calculate the spectral densities for a methylene deuteron, one needs to solve equation (19) to give $p_{il_0}(t)$. This is done by symmetrizing $\tilde{R}$ and then diagonalizing to obtain N real and negative eigenvalues Λ_n and eigenvectors $\mathbf{x}^n$, from which

$$p_{il_0}(t) = x_i^{(1)}(x_l^{(1)})^{-1}\sum_{n=1}^{N} x_i^{(n)}x_l^{(n)}\exp(-|\Lambda_n|t). \tag{23}$$

In the decoupled model, the spectral densities $J^{(i)}_{m_L}(m_L\omega)$ of the C_i deuteron(s) for $m_L \neq 0$ are given by

$$J^{(i)}_{m_L}(m_L\omega) = \frac{3\pi^2}{2}(q^{(i)}_{CD})^2 \sum_{m_M}\sum_{n=1}^{N} c_{m_L m_M}\left|\sum_{l=1}^{N} d^2_{m_N 0}(\beta^{(i)l}_{N,Q}) d^2_{m_M m_N}(\theta) \times \exp[-im_N(\alpha^{(i)l}_{N,Q} + 90°)] x^{(1)}_l x^{(n)}_l\right|^2 \times \sum_j a^{(j)}_{m_L m_M}[(\tau^{(j)}_{m_L m_M})^{-1} + |\Lambda_n|]/\{(m_L\omega)^2 + [(\tau^{(j)}_{m_L m_M})^{-1} + |\Lambda_n|]^2\}, \quad (24)$$

where $\beta^{(i)l}_{N,Q}$ and $\alpha^{(i)l}_{N,Q}$, the polar angles of the C_i–D bond of the lth conformer in the N frame, are by-products of equation (17), and the rotational correlation times $\tau^{(j)}_{m_L m_M}$ are given in the model of Nordio by

$$\tau^{(j)}_{m_L m_M} = b^{(j)}_{m_L m_M}/[6D_\perp + m^2_M(D_\parallel - D_\perp)], \quad (25)$$

with $D_\parallel$ and $D_\perp$ being the rotational diffusion constant of an 'average' conformer about its principal long axis and the diffusion constant of this axis $a^{(j)}_{m_L m_M}$ and $b^{(j)}_{m_L m_M}$ represent, respectively, normalized relative weights and decay time constants in multi-exponentials of the correlation functions, and $c_{m_L m_M}$ are the mean squares of the Wigner rotation matrices. The a, b, and c coefficients depend on the order parameter $\langle P_2\rangle$ and are tabulated [12] for a Maier–Saupe potential.

Assuming free internal ring rotation in the strong collision limit, the spectral densities for the ring deuterons are

$$J^{(R)}_{m_L}(m_L\omega) = \frac{3\pi^2}{2}(q^{(R)}_{CD})^2 \sum_{m_M}\sum_{m_R} c_{m_L m_M}[d^2_{m_R 0}(\beta_{R,Q})]^2[d^2_{m_M m_R}(\beta_{M,R})]^2 \times \sum_j a^{(j)}_{m_L m_M}[(\tau^{(j)}_{m_L m_M})^{-1} + (1-\delta_{m_R 0})D_R]/\{(m_L\omega)^2 + [(\tau^{(j)}_{m_L m_M})^{-1} + (1-\delta_{m_R 0})D_R]^2\}, \quad (26)$$

where $\beta_{R,Q}$ is the angle between the C–D bond and the biphenyl *para*-axis, $\beta_{M,R}$ is the angle between the *para*-axis and the z_M axis, and D_R is a rotational diffusion constant for ring rotations. The fitting quality factor Q in the spectral density calculation is given by the per cent mean-squared deviation

$$Q = \frac{\sum_{\omega_0}\sum_i\sum_{m_L}[J^{(i)}_{m_L}(\text{expt}) - J^{(i)}_{m_L}(\text{calc})]^2}{\sum_{\omega_0}\sum_i\sum_{m_L}[J^{(i)}_{m_L}(\text{expt})]^2} \times 100. \quad (27)$$

3. Experimental

The perdeuteriated 6OCB-d_{21} sample was purchased from Merck Sharp and Dohme, Canada Ltd. and has a clearing temperature T_C of 75°C. Deuterium T_{1Z} and T_{1Q} were measured with a home-built superheterodyne coherent pulsed NMR spectrometer operating for deuterons at 15·3 and 46·05 MHz with a Varian 15 in. electromagnet and a 7·1 Tesla Oxford magnet, respectively. The sample was placed in a NMR probe whose temperature was regulated by an air flow with a Bruker BST-1000 temperature controller or by an external oil bath circulator. The temperature of the NMR probe was calibrated using quadrupolar splittings of a liquid crystal whose transition temperature were known. The temperature gradient across the sample was estimated to be better

than 0·3°C. The $\pi/2$ pulse width of *c.* 4·5 μs was produced by a model 200L (Amplifier Research) power amplifier. Pulse control, signal acquisition, Fourier transform and data processing were performed [33] using a General Electric 1280 computer. The broadband Jeener–Broekaert excitation sequence (see figure 1 (*c*)) was used to measure simultaneously the Zeeman and quadrupolar spin-lattice relaxation times. The sequence was appropriately phase-cycled [34, 35] through radiofrequency and receiver phases to get rid of the unwanted double quantum coherence and r.f. phase imperfections. Signal acquisition was started *c.* 10 μs after each monitoring $\pi/4$ pulse, and averaged over 240–1600 scans at 15·3 MHz and over 32–128 scans at 46·05 MHz depending on the signal strengths of various resolvable sites (see figure 1 (*b*)). Despite broadband excitation of quadrupolar order, several experiments were performed at each temperature because of large differences in relaxation rates among various deuterons. A typical deuterium NMR spectrum of 6OCB-d_{21} with peak assignments [21] is shown in figure 1 (*b*). The signals from the ring R' and methyl deuterons are strongly overlapped except at the low temperature end of the nematic range (40°C). In the present study, the ring R' is excluded because of the severe overlap [23]. Since the relaxation times of the methyl group were much longer than those of the ring, they were determined by looking at delays longer than *c.* 40 ms. A deconvolution routine was employed to obtain the areas under the two partially overlapped peaks, 3 and 4. Each line was

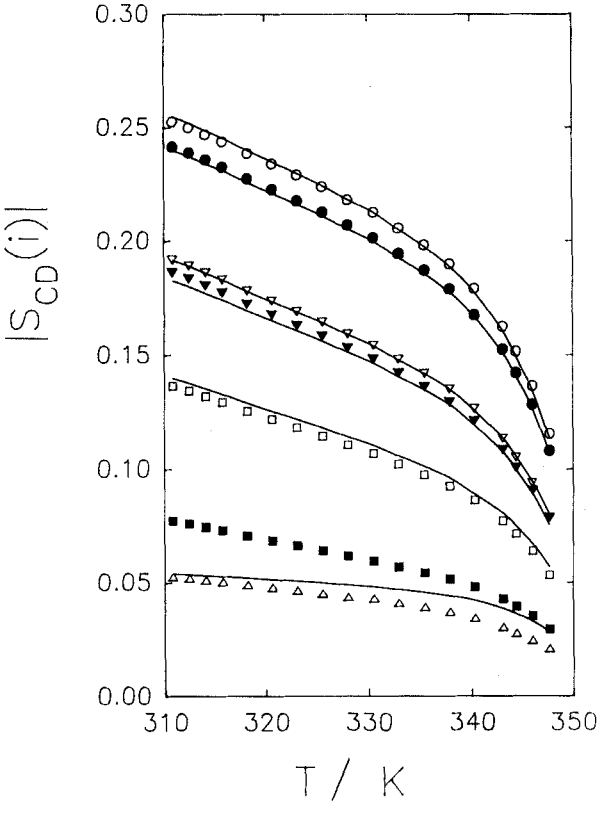

Figure 2. Plots of experimental segmental order parameter $S_{CD}^{(i)}$ versus temperature. Solid curves are theoretical fits to the data. ○, ▽, □ denote C_1, C_3 and C_5 data, while their corresponding solid symbols denote C_2, C_4 and C_6, respectively, and △ the ring R data.

assumed to be 100 per cent gaussian in shape. The procedures for data reductions to give T_{1Z} and T_{1Q} have been described elsewhere [18, 32]. The experimental uncertainty in the spin-lattice relaxation times was estimated to be ± 5 per cent or better. The quadrupolar splittings were determined from deuterium NMR spectra obtained by Fourier transforming the FID signal after a $\pi/2$ pulse. These splittings had an experimental error of better than ± 1 per cent.

4. Results and discussion

4.1. *Orientational order parameters*

In this section, we describe the results of fitting the segmental order parameters $S_{CD}^{(i)}$ of the ring R and methylene deuterons according to equation (11). Figure 2 shows the experimental $S_{CD}^{(i)}$ as a function of temperature. We use Amoeba to minimize f and obtain $U(n, \omega)$ in terms of E_{tg}, X_a and $\lambda_x = X_{cc}/X_a$. We allowed both E_{tg} and $\angle$COC to vary initially, but decided to fix the $\angle$COC at 126°, a value that was used for the nO.m series [29]. The orientations of the chain were determined by the first dihedral angle at the junction with the biphenyl ring, which also sampled three RIS (0, $\pm 112°$). We found that when this dihedral angle took the values of 30°, 90° and 150°, the f values were improved, but the relaxation data seemed to disfavour this choice (see below). We fixed the value of E_{tg} at 3800 J mol^{-1} [21] as suggested by Counsell *et al.*, though a slightly higher value would improve the fits somewhat. However, we let λ_x vary with temperature, while Counsell *et al.*, adopted a constant value of 0·13 for this

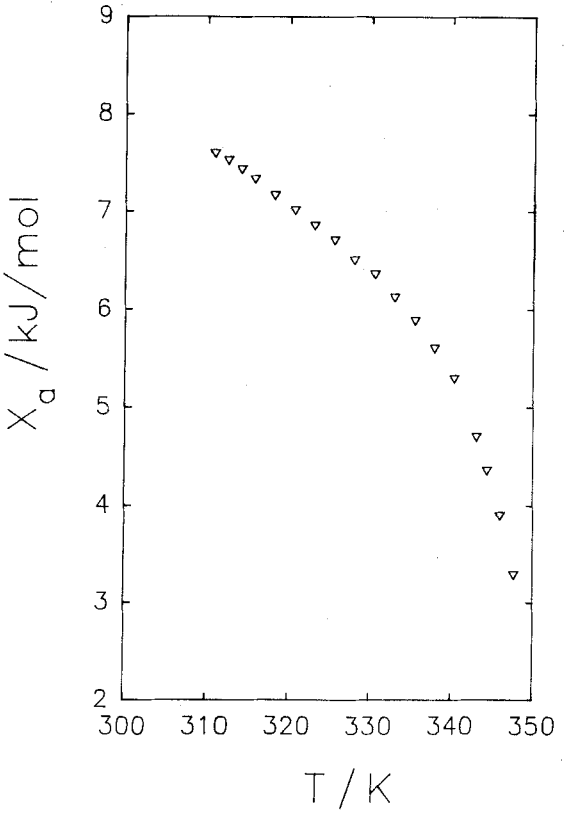

Figure 3. Plot of the core interaction parameter X_a versus temperature.

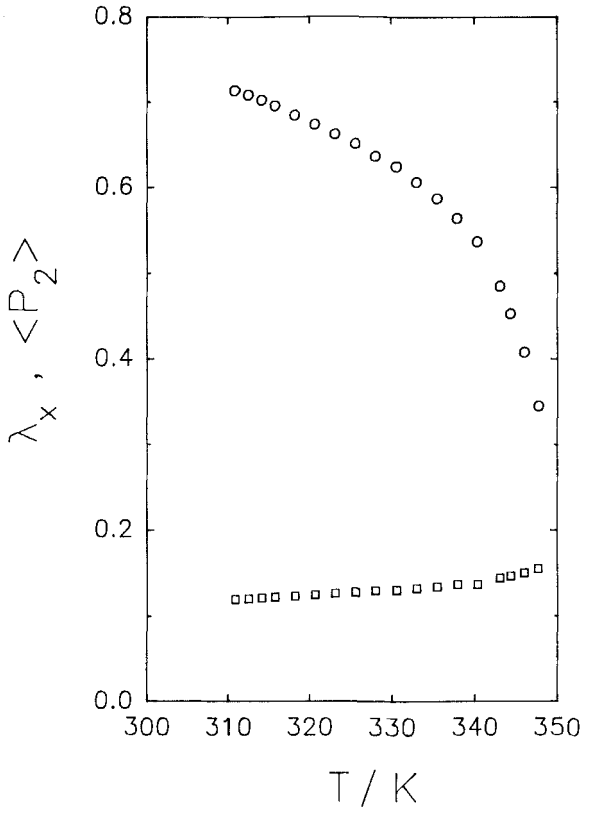

Figure 4. Plots of $\langle P_2 \rangle$ and λ_x versus temperature. The $\langle P_2 \rangle$ is the order parameter derived for the 'average' conformer of the 6OCB molecule. ○ and □ denote $\langle P_2 \rangle$ and λ_x, respectively.

parameter. With E_{tg} fixed ($E_{g^{\pm}g^{\mp}} = 0$), a two-parameter fit was carried out at each temperature, resulting in sum squared errors of the order of 10^{-5} over the entire nematic range. The theoretical $S_{CD}^{(i)}$ curves from the additive potential method are also shown in figure 2. No theoretical curve for the methyl group is shown, as its splitting was not included in the minimization. It can be seen that the fitting is poor for the ring at higher temperature. Also there is a systematic deviation between the theory and experimental $S_{CD}^{(5)}$. This could be improved somewhat if the CD angle for the ring was changed from the present 59° to 58·8° and the first dihedral angle was set at 30°, 90° and 150°. However, such refinement was abandoned. The model parameters X_a and λ_x, as a function of temperature, are shown in figure 3 and 4, respectively. Our X_a values are almost identical to those obtained by Counsell *et al.* [21], but these cover a wide temperature range. It can be seen that the X_a decrease from 7·92 kJ mol^{-1} at 311 K at 3·34 kJ mol^{-1} at T_c. Our λ_x increases with temperature from 0·115 to 0·155 at T_c. This would imply that X_{cc} has a slightly stronger temperature dependence than X_a, as found for 5CB [20] and MBBA [18]. The variation of order parameter $\langle P_2 \rangle$ for the average conformer with temperature (0·73 at 311 K to 0·35 at 348 K) is also shown in figure 4. This parameter can be obtained by calculating the conformationally averaged order matrix $\langle \tilde{S} \rangle$ [24] from $p_{eq}(n)$ and $S_{\alpha\beta}^{n}$. The principal axes (x_p, y_p, z_p) can be found by diagonalizing the $\langle \tilde{S} \rangle$ whose principal components are $\langle P_2 \rangle$ and $\langle S_{xx} \rangle - \langle S_{yy} \rangle$.

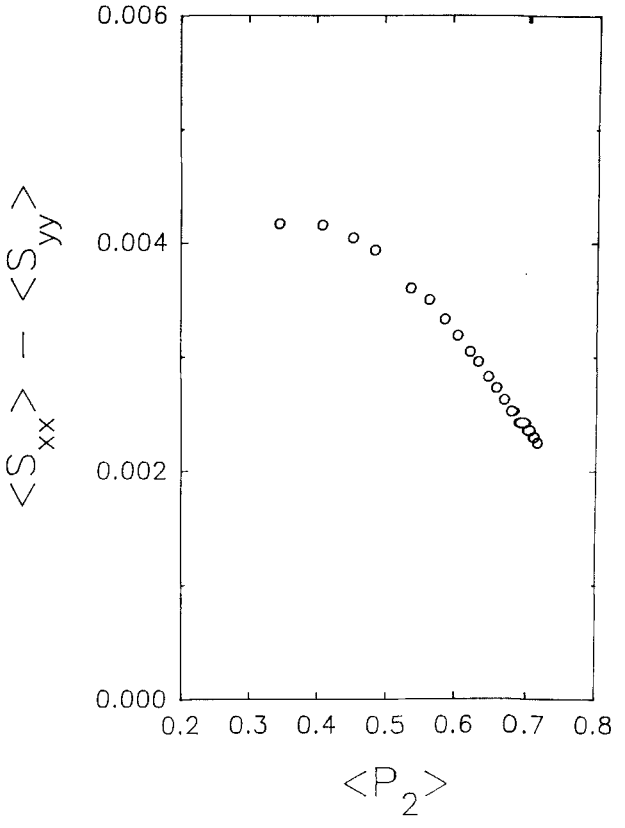

Figure 5. Plot of the average biaxial order parameter ($\langle S_{xx}\rangle - \langle S_{yy}\rangle$) versus $\langle P_2\rangle$.

We found that $\langle S_{xx}\rangle - \langle S_{yy}\rangle$ is very small and its temperature variation is shown in figure 5. Near T_c its value is nearly constant at *c.* 0·004. In comparison with MBBA [18] and 5CB [20], the magnitude of $\langle S_{xx}\rangle - \langle S_{yy}\rangle$ seems to decrease with increasing chain length. This would imply that the longer the molecule, the more its 'average' shape tends to be like a rod. The z_p axis of the average conformer is found to lie very close to the ring *para*-axis ($< 0{\cdot}2°$ at 311 K; this angle decreases to 0·09° close to T_c). Thus the ring *para*-axis will be treated as the long diffusion axis of the molecule. We note here that the additive potential method is sufficient to predict the ordering matrices $S^n_{\alpha\beta}$ and the conformational probabilities $p_{eq}(n)$ for the purpose of treating the relaxation data.

4.2. *Correlated chain dynamics*

Figure 6 presents the experimental spectral density data at 15·3 (open symbols) and 46·05 MHz (closed symbols) for the ring and C_3 deuterons (see figure 7 (*a*)), for C_1 and C_5 deuterons (see figure 7 (*b*)), for C_2 deuterons (see figure 7 (*c*)) and for C_4 and C_6 deuterons (see figure 7 (*d*)). It is seen that both $J_1(\omega)$ and $J_2(2\omega)$ are frequency dependent. Except for the ring deuterons, the frequency dependence of $J_1(\omega)$ is much larger than that of $J_2(2\omega)$. Also the J_1s are always larger than the corresponding J_2s, except that at 46 MHz, the $J_1(\omega_0)$ and $J_2(2\omega_0)$ are roughly equal at low temperatures. All spectral densities decrease with increasing temperature. This is a common feature

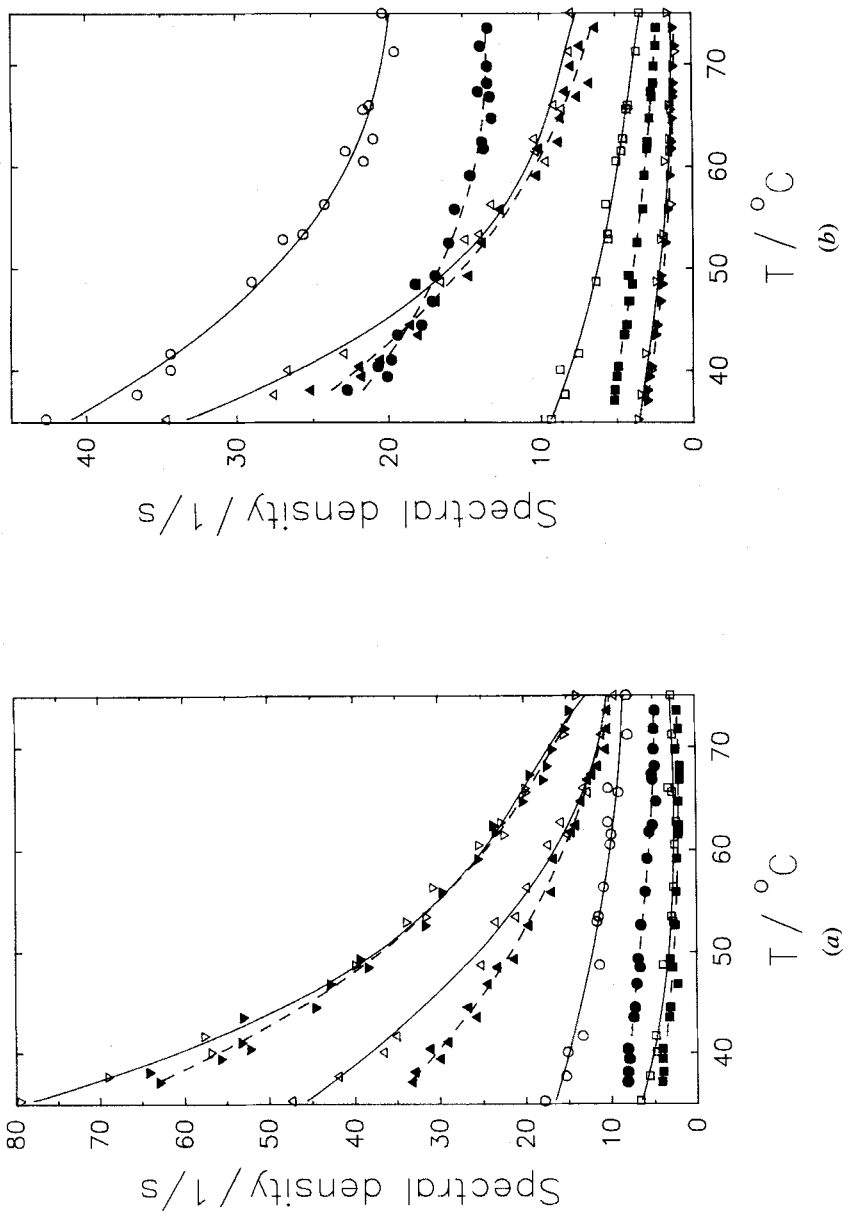

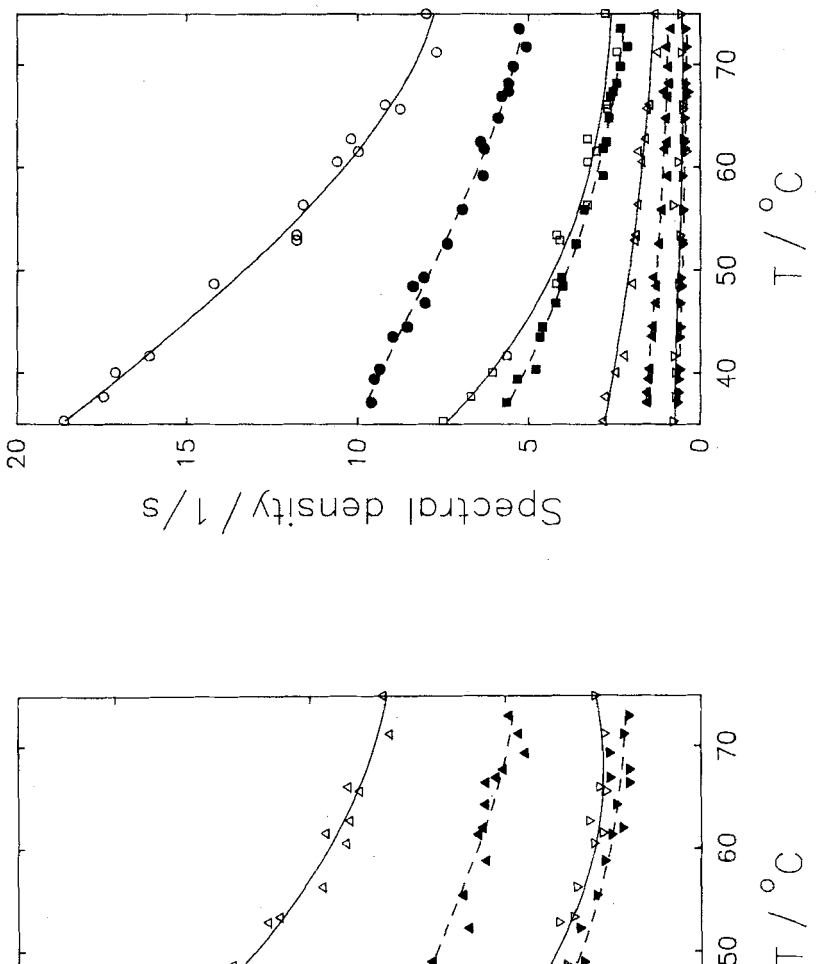

Figure 6. Plots of spectral densities versus temperature in the nematic phase of 6OCB-d_{21}. Open symbols denote data collected at 15·3 MHz and closed symbols at 46·05 MHz. ▽ and △ denote $J_1(\omega)$ and $J_2(2\omega)$ for the ring deuterons, while ○ and □ denote $J_1(\omega)$ and $J_2(2\omega)$ for C_3 deuterons (*a*). ○ and △ denote $J_1(\omega)$ and $J_2(2\omega)$ for C_1 deuterons, while □ and ▽ denote $J_1(\omega)$ and $J_2(2\omega)$ for C_5 deuterons (*b*). △ And ▽ denote $J_1(\omega)$ and $J_2(2\omega)$ for C_2 deuterons (*c*). ○ and □ denote $J_1(\omega)$ and $J_2(2\omega)$ for C_4 deuterons, while △ and ▽ denote $J_1(\omega)$ and $J_2(2\omega)$ for C_6 deuterons (*d*). The solid curves are drawn to aid the eye and are used for fits in the decoupled model.

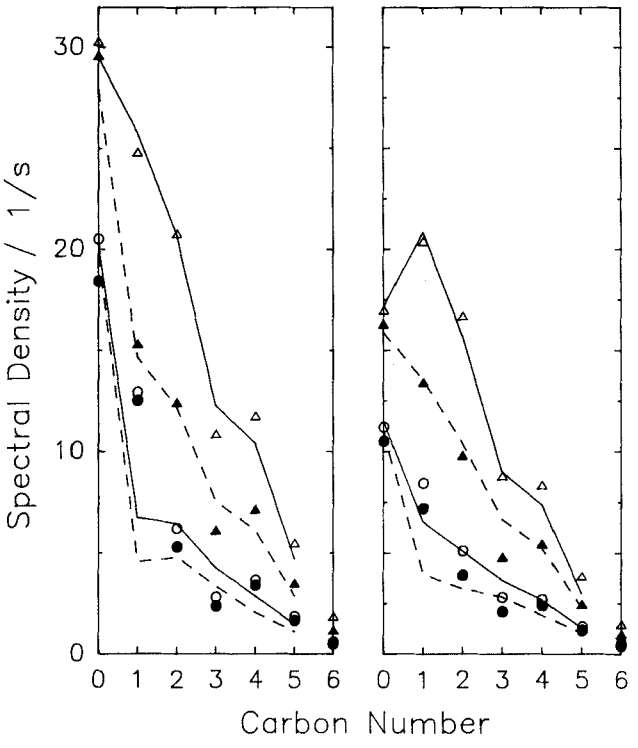

Figure 7. Plots of spectral densities $J_1(\omega)$ (△) and $J_2(2\omega)$ (○) versus the carbon number at 328 K (left) and 343 K (right). Carbon 0 refers to ring deuterons. Solid (15·3 MHz) and dashed (46·05 MHz) lines are calculated spectral densities based on model fitting. Open and closed symbols denote 15·3 and 46·05 MHz data, respectively. Error bars for the data could be estimated from the scattering of data from the smooth curves in figure 6.

to all thermotropic liquid crystals. The site dependence of spectral densities is shown for two different temperature (328 K and 343 K) in figure 7.

Quantitative fits between experimental spectral densities at both frequencies and their theoretical counterparts given by equations (24)–(26) were attempted at three different temperatures by means of Amoeba. The methyl data were not used in the minimization, since motion of the group is more complex [15] due to fast rotations about the methyl symmetry axis. There are six model parameters to be determined at each temperature from twelve J_1s (six from each frequency) and twelve J_2s. We summarize the derived model parameters and the Q-factor in the table. The Q-factors show that the decoupled model of correlated internal motion is qualitatively correct. Moreover, the rotational diffusion constants appear to show the expected thermally activated behaviour. The apparent activation energy for $D_\perp$ seems small, but this may be due to the inability to determine precisely this particular motion from spectral density measurements [19]. The jump rate constant k_3 is the largest which is consistent with the three-bond motion being a kink-type motion of the chain. In modelling the spectral density data, we found that the ks are very sensitive to slight variations in the experimental spectral densities. We therefore would not remark further on these parameters. To illustrate our model, the theoretical predictions at 328 and 343 K are also

Motional parameters derived from spectral density measurements at 15·3 and 46·05 MHz using the decoupled model.

T/K	$k_1/\times 10^{13}\,s^{-1}$	$k_2/\times 10^{13}\,s^{-1}$	$k_3/\times 10^{14}\,s^{-1}$	$D_\perp/\times 10^{7}\,s^{-1}$	$D_\parallel/\times 10^{9}\,s^{-1}$	$D_R/\times 10^{9}\,s^{-1}$	Q-factor/%
343	0·28	6·94	2·90	4·67	1·97	5·03	1·4
338	2·68	0·81	5·64	3·96	1·46	4·44	1·5
328	4·29	0·78	3·01	3·25	0·73	3·39	2·8

presented in figure 7. Their Q-values are given in the table. The model seems to give a poorer Q-factor at a lower temperature. The serious discrepancy is the low $J_2(2\omega)$ values predicted for C_1. Indeed, we tried to change the first dihedral angle of the chain to 30°, 90° and 150°, and found that the fits to both J_1 and J_2 were very poor for C_1. Thus it would appear that this particular dihedral angle must be picked carefully. No attempt to do this was made here, because one must await calculations that use all 729 conformations. We also note that the predicted site dependence of spectral densities at the C_3 and C_4 is contrary to the experimental trend. Given the many assumptions used in the decoupled model and the limited number of conformations, the model can produce qualitative agreement with experimental spectral densities for a molecule which has a chain of seven atoms.

In conclusion, we have used a model of correlated internal motion to explain consistently the quadrupolar splittings and spectral densities of motion of 6OCB. The use of the pentane effect to limit the size of the transition matrix does not seem to present a major concern, as the derived rotational diffusion constants and the jump rate constants for one-, two- and three-bond motions all appear to be physically reasonable. A more sophisticated model and/or the elimination of the pentane effect may be required if one wants to predict more accurately the site dependences of $J_1(\omega)$ and $J_2(2\omega)$.

We are grateful to Dr G. M. Richards for her contribution in computer programming, and to Mr D. Bramadat and Mr N. Finlay for their technical support. The financial support of the Natural Sciences and Engineering Council of Canada is gratefully acknowledged. The partial support in the acquisition of the 7·1 Tesla magnet from Brandon University is highly appreciated.

References

[1] DONG, R. Y., 1994, *Nuclear Magnetic Resonance of Liquid Crystals* (Springer-Verlag).
[2] VOLD, R. R., 1985, *Nuclear Magnetic Resonance of Liquid Crystals*, edited by J. W. Emsley (D. Reidel Publishing Co.).
[3] BECKMANN, P. A., EMSLEY, J. W., LUCKHURST, G. R., and TURNER, D. L., 1983, *Molec. Phys.*, **50,** 699.
[4] BARBARA, T. M., VOLD, R. R., and VOLD, R. L., 1983, *J. chem. Phys.*, **79,** 6338.
[5] DONG, R. Y., and SRIDHARAN, K. R., 1985, *J. chem. Phys.*, **82,** 4838.
[6] GOLDFARB, D., DONG, R. Y., LUZ, Z., and ZIMMERMAN, H., 1985, *Molec. Phys.*, **54,** 1185.
[7] DONG, R. Y., EMSLEY, J. W., and HAMILTON, K., 1989, *Liq. Crystals*, **5,** 1019.
[8] HOATSON, G. L., TSE, T. Y., and VOLD, R. L., 1992, *J. magn. Reson.*, **98,** 342.
[9] GOETZ, J. M., HOATSON, G. L., and VOLD, R. L., 1992, *J. chem. Phys.*, **97,** 1306.
[10] NORDIO, P. L., and BUSOLIN, P., 1971, *J. chem. Phys.*, **55,** 5485. NORDIO, P. L., RIGATTI, G., and SEGRE, U., 1972, *J. chem. Phys.*, **56,** 2117; 1973, *Molec. Phys.*, **25,** 129.
[11] POLNASZEK, C. F., BRUNO, G. V., and FREED, J. H., 1973, *J. chem. Phys.*, **58,** 3185. POLNASZEK, C. F., and FREED, J. H., 1975, *J. phys. Chem.*, **79,** 2283.
[12] VOLD, R. R., and VOLD, R. L., 1988, *J. chem. Phys.*, **88,** 1443.
[13] BECKMANN, P. A., EMSLEY, J. W., LUCKHURST, G. R., and TURNER, D. L., 1986, *Molec. Phys.*, **59,** 97.
[14] DONG, R. Y., and RICHARDS, G. M., 1990, *Chem. Phys. Lett.*, **171,** 389. DONG, R. Y., 1991, *Phys. Rev.*, **43,** 4310.
[15] FERRARINI, A., MORO, G. J., and NORDIO, P. L., 1990, *Liq. Crystals*, **8,** 593.
[16] PINCUS, P., 1969, *Solid St. Commun.*, **7,** 415. VOLD, R. R., and VOLD, R. L., 1988, *J. chem. Phys.*, **88,** 4655.
[17] KÖLLNER, R., SCHWEIKERT, K. H., and NOACK, F., 1993, *Liq. Crystals*, **13,** 483.
[18] DONG, R. Y., FRIESEN, L., and RICHARDS, G. M., 1994, *Molec. Phys.*, **81,** 1017.

[19] DONG, R. Y., and RICHARDS, G. M., 1992, *J. chem. Soc. Faraday Trans.*, **88,** 1885. DONG, R. Y., and RICHARDS, G. M., 1992, *Chem. Phys. Lett.*, **200,** 54.
[20] RICHARDS, G. M., and DONG, R. Y. (in preparation).
[21] COUNSELL, C. J. R., EMSLEY, J. W., LUCKHURST, G. R., and SACHDEV, H. S., 1988, *Molec. Phys.*, **63,** 33.
[22] POON, C. D., WOOLDRIDGE, C. M., and FUNG, B. M., 1988, *Molec. Crystals liq. Crystals*, **157,** 303.
[23] DONG, R. Y., and O'BANNON, G. W., 1991, *Molec. Crystals liq. Crystals*, **209,** 139.
[24] FLORY, P. J., 1969, *Statistical Mechanics of Chain Molecules* (Interscience).
[25] COUNSELL, C. J. R., EMSLEY, J. W., HEATON, N. J., and LUCKHURST, G. R., 1985, *Molec. Phys.*, **54,** 847.
[26] EMSLEY, J. W., LUCKHURST, G. R., and STOCKLEY, C. P., 1982, *Proc. R. Soc.* A, **381,** 117.
[27] PRESS, W. H., FLANNERY, B. P., TENKOLSKY, S. A., and VETTERLING, W. T., 1986, *Numerical Recipes* (Cambridge University Press), p. 292.
[28] JACOBSEN, J. P., BILDSOE, H. K., and SCHUMBERG, K., 1976, *J. magn. Reson.*, **23,** 153. AHMAD, S. B., PACKER, K. J., and RAMSDEN, J. M., 1977, *Molec. Phys.*, **33,** 857. VOLD, R. R., and VOLD, R. L., 1977, *J. chem. Phys.*, **66,** 4018.
[29] CHENG, G. Q., and DONG, R. Y., 1988, *J. chem. Phys.*, **89,** 3308.
[30] ELLIS, D. M., and BJORKSTAM, J. L., 1967, *J. chem. Phys.*, **46,** 4460.
[31] LUCKHURST, G. R., ZANNONI, C., NORDIO, P. L., and SEGRE, U., 1975, *Molec. Phys.*, **30,** 1345.
[32] VALEUR, B., JARRY, J. P., GENY, F., and MONNERIE, L., 1975, *J. polym. Sci.*, **13,** 667; 1975, *Ibid.*, **13,** 675.
[33] DONG, R. Y., and RICHARDS, G. M., 1988, *J. chem. Soc. Faraday Trans.*, **84,** 1053.
[34] VOLD, R. L., DICKERSON, W. H., and VOLD, R. R., 1981, *J. magn. Reson.*, **43,** 213.
[35] DONG, R. Y., 1992, *Bull. magn. Reson.*, **14,** 134.